Available online at www.sciencedirect.com

jmr&t Journal of Materials Research and Technology

journal homepage: www.elsevier.com/locate/jmrt

Original Article

Micro/nano-structure leads to super strength and excellent plasticity in nanostructured 304 stainless steel

Jie Sheng [a,b,c], *Jiafu Wei* [a], *Zhengning Li* [d], *Kun Man* [a], *Weiqian Chen* [a,c], *Guocai Ma* [a,b], *Yuehong Zheng* [a], *Faqi Zhan* [a], *Peiqing La* [a,*], *Yanchun Zhao* [a,**], *Abdelrahim Husain* [e]

[a] *State Key Laboratory of Gansu Advanced Non-Ferrous Metal Materials, Lanzhou University of Technology, Lanzhou, 730050, China*

[b] *Jiuquan Iron and Steel (Group) Co., Ltd., Jiayuguan, 735100, China*

[c] *Gansu Key Laboratory of Solar Power System Engineering Project, Jiuquan Vocational and Technical College, Jiuquan 735100, China*

[d] *School of Materials Science and Engineering, Lanzhou Jiaotong University, Lanzhou, 730070, China*

[e] *Department of Physics, Faculty of Science and Technology, University of Shendi, Shendi, River Nile State, P.O. Box 407, Sudan*

ARTICLE INFO

Article history:
Received 1 October 2021
Accepted 27 December 2021
Available online 12 January 2022

Keywords:
Micro/nano-structure
304 stainless steel
Strength-plasticity
Heterogeneous composite structure

ABSTRACT

Micro/nano-structure is one of the important types of multilayer construction, which can make nanocrystalline metals and alloys with excellent comprehensive mechanical properties. By means of Aluminothermic Reaction (AR) and subsequent rolling with deformation of 50% at room temperature (RT) and followed by annealed at 973 K for 1 h, a heterogeneous composite structure of micro/nano-structured 304 stainless steel (SS) is obtained. Such a stainless steel specimen exhibits a tensile strength as high as 1023 MPa and an elongation-to-failure of about 27.3%. In the process, the much elevated strength originates from martensite strengthening, austenite grain refinement and dislocation density increasing, while ductility promotes from the recrystallization of deformed austenite and recovery of strain induced martensite. Superior strength–ductility combination achieves in micro/nano-structured 304 SS, which demonstrates a novel approach for optimizing the mechanical properties in engineering materials.

* Corresponding author.
** Corresponding author.
E-mail addresses: pqla@lut.cn (P. La), yczhao@lut.cn (Y. Zhao).

https://doi.org/10.1016/j.jmrt.2021.12.117

1. Introduction

304 stainless steel (SS) (0Cr18Ni9) was a kind of universal stainless steel. It was widely used in aerospace, chemical energy, automobile industry, shipbuilding, food, medical industry and other fields [1–3]. The modern industry had put forward a higher demand for 304 SS, and the research of high strength and high plastic steel had become a great focus in recent years [4–7].

It had been found that biomaterials with excellent comprehensive mechanical properties always had more complex structural features [8,9], such as uneven geometry [10], spatial distribution [11], multi-scale, non-uniform tissues distribution [12] and multi-level coupling structure [13], etc. They could effectively overcome performance defects of single homogeneous ultrafine/nanocrystalline structure materials and significantly improved plastic deformation ability [14,15]. The unique micro/nano-structure of biomaterials had become a source of innovation in the design and preparation of new composite materials [16,17]. Micro/nano-structure was one of the important types of multilayer construction [18–20]. Herein, we reported a micro/nano-structured 304 SS which was achieved the imhomogeneous structure via Aluminothermic Reaction (AR) experiments [21–23], and subsequent different rolling and annealing schedule to control different microstructures. This micro/nano-structured 304 SS achieved the best match between strength and plasticity.

2. Materials and experimental procedure

In the present work, the initial 304 SS synthesized via AR with 5 MPa controlled atmosphere in argon gas. The experimental details information on the processing had been reported in Ref. [24–26]. The chemical composition of 304 SS used in this investigation was shown in Table 1. The big ingot was processed and cut into a strip of 100 × 50 × 5 mm^3 with a wire cutter. The 304 SS strip was performed rolling for deformation of 50% at RT and followed by annealed at 973 K for 1 h to assure combination of super strength and excellent plasticity. The rolling thickness reduction was 50% and the corresponding specimen was thinned from 5 mm to 2.5 mm. The plate thickness variation was presented in Fig. 1 before and after rolling.

All microstructures were analyzed in the transverse plane of the 304 SS sheet, and through thickness plane was perpendicular to the rolling direction. Microstructural characterization was carried out using scanning electron microscope (SEM, JSM-6700F) with a secondary electron detector and transmission electron microscope (TEM, JEM-2010). Electron backscatter diffraction (EBSD) analysis was performed using a field emission scanning electron microscope, Quanta 450 FEG SEM (equipped with aztecx-max80 probe). The EBSD data analysis was performed with HKL Channel 5 software. The specimens for EBSD analyses should be electropolished in 8 pct perchloric acid alcohol solution. A mixture of 45 ml HCl+60 ml H_2O+10g $FeCl_3$ was etched for 30 s to reveal the microstructure for optical and conventional SEM specimens. For TEM observation, thin foils were mechanically ground to a thickness of 50 μm followed by electrochemical thinning using a twin-jet electro-polishing device in a solution of 5 vol. % perchloric acid in ethanol. The dog-bone shaped tensile test specimens were wire-cutting machined from a target 304 SS sheet with the dimension as shown in Fig. 2, and the thickness was 1 mm. Uniaxial tensile tests were carried out at RT by a AT10t universal mechanical testing machine with a maximum loading capacity of 100 kN operating at a crossing speed of 0.2 mm/min. The tensile direction was parallel to the rolling direction.

Table 1 – Chemical compositions of 304 SS studied in this study (wt.%).

C	Si	Mn	Cr	Ni	Fe
0.05	0.60	1.20	18.00	10.00	Bal.

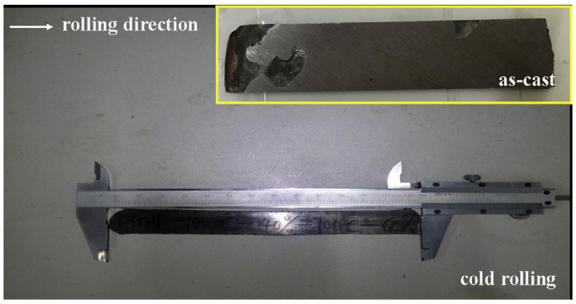

Fig. 1 – The marco image of 304 SS before and after rolling.

3. Results

3.1. Microstructural characterization

The studied 304 SS was produced by the means of AR, and cool rolling with a 50% deformation at RT, then followed by annealing at 973 K for 1 h. Metallographic microstructures of three different thickness 304 SS were provided in Fig. 3. According to the X-ray diffraction (XRD) analysis, crystalline structure of as-cast 304 SS was mainly face centered cubic (fcc) austenite in Fig. 3(a). The microstructure after cold rolling was composed of austenite and martensite. Most of the white areas were austenite and the black strip structure was strain induced martensite. Grains were obviously elongated along

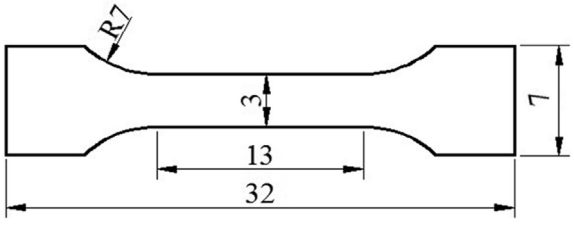

Fig. 2 – Schematic illustration of tensile specimen (unit: mm).

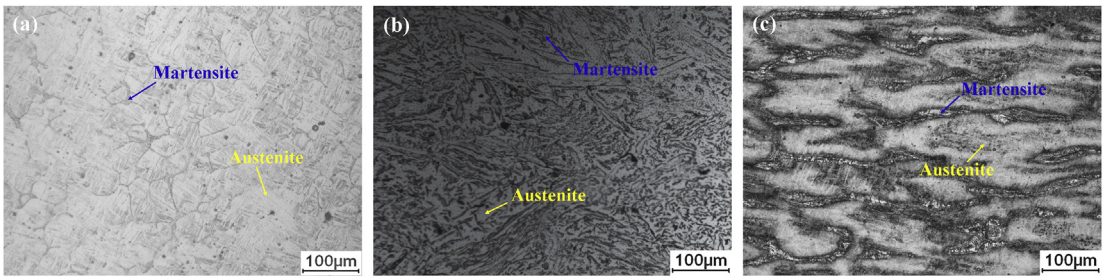

Fig. 3 – Typical metallographic microstructure of 304SS (a) as-cast, (b) cold rolling with a thickness reduction of 50% at RT, (c) followed by annealing at 973 K for 1 h.

the rolling direction, and deformation of each grain also presented non-uniformity, as shown in Fig. 3(b). The content of a large number of linear strain induced martensite was 29.1% via IPWIN6 software. After annealing, the volume fraction of martensite decreased to 17.6% in Fig. 3(c). The strength of alloy always decreases with the decrease of martensite content. The rule is also reflected in Figs. 3(b) and (c).

Orientation imaging microscopy (OIM) of austenite region for 304 SS before and after annealing was illustrated in Fig. 4, respectively. It could be seen from OIM that most austenite grains were (111) oriented in Fig. 4(a), while (101) orientation was significantly larger after annealing in Fig. 4(b).

After annealing, the micro/nano-structured features of 304 SS were obtained and given as shown in Fig. 5. Fig. 5(a) presented the typical SEM image, RD represented the rolling direction. It could be seen that protuberance was austenite phase, while hole was martensite phase. That's because, austenite was less resistant to corrosion here, and the martensite phase was strain induced martensite. It could be seen from OIM in Fig. 4(b) that the number of grains with (101) orientation was significantly larger, and formed obvious {112}<101> texture in corresponding inverse pole figure of Fig. 5(b). After cold rolling, austenite had no time to occur recrystallization and mainly forms deformation texture. At this time, the main type of texture was copper texture {112}<111>, and the texture strength in {112}//ND direction becomes larger. The microstructure of specimen changed via annealing. A part of the grains grow up by annealing, which made the specimen had better elongation strength matching. {112}<101> texture was significantly enhanced after annealing. That was because soft phases around hard phases were easy to form shear zone and deformation zone in the deformation process. The deformation energy was high in these places, where {112}<101> grains would nucleate preferentially. Fig. 5(c) showed grain size distribution that the number of ultrafine grains below 1 μm accounted for about 82.5%. The volume fraction of austenite grains with average grain size less than 300 nm was 38.8%, and the average grain size of austenite was 713.8 nm. Fig. 5(d) and Fig. 5(e) were the distribution diagram of grain boundary state and statistical diagram of grain boundary misorientations. It could be observed that the green small angle grain boundary still accounted for the majority after annealing from Fig. 5(d). As we could sum from the statistical results of Fig. 5(e), the small angle grain boundary with ferrite was less than 15° and accounted for 80.9%, in which the sub grain boundary with ferrite less than 2° accounted for 42.1%. Distribution of recrystallized grains, substructures and deformed grain were showed in Fig. 5(f), EBSD analysis results of Channel 5 software specimens were used, and volume of recrystallized grains and the deformed grains was 5.7% and 87.6%, respectively. TEM was used to characterize austenite grains at about 100 nm more clearly. Fig. 5(g) and Fig. 5(h) provided bright field and dark field TEM images, respectively. Corresponding selected area electron diffraction (SAED) was inserted in bright field (Fig. 5(g)). The defects such as tangled dislocations and stacking faults could be observed in TEM images. According to results of SAED, black particles were nanocrystalline austenite phases, and white bright areas were micron austenite phases. Statistical analysis showed the average grain size of nanocrystalline and ultrafine austenite was 86 nm, accounting for 21% of bright field images, which was consistent with results of EBSD images. The amount of

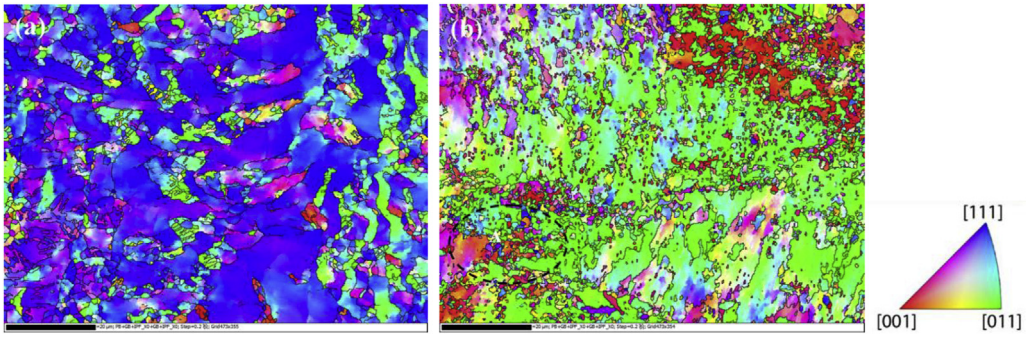

Fig. 4 – OIM image showed austenite region of 304 SS, (a) before and (b) after annealing.

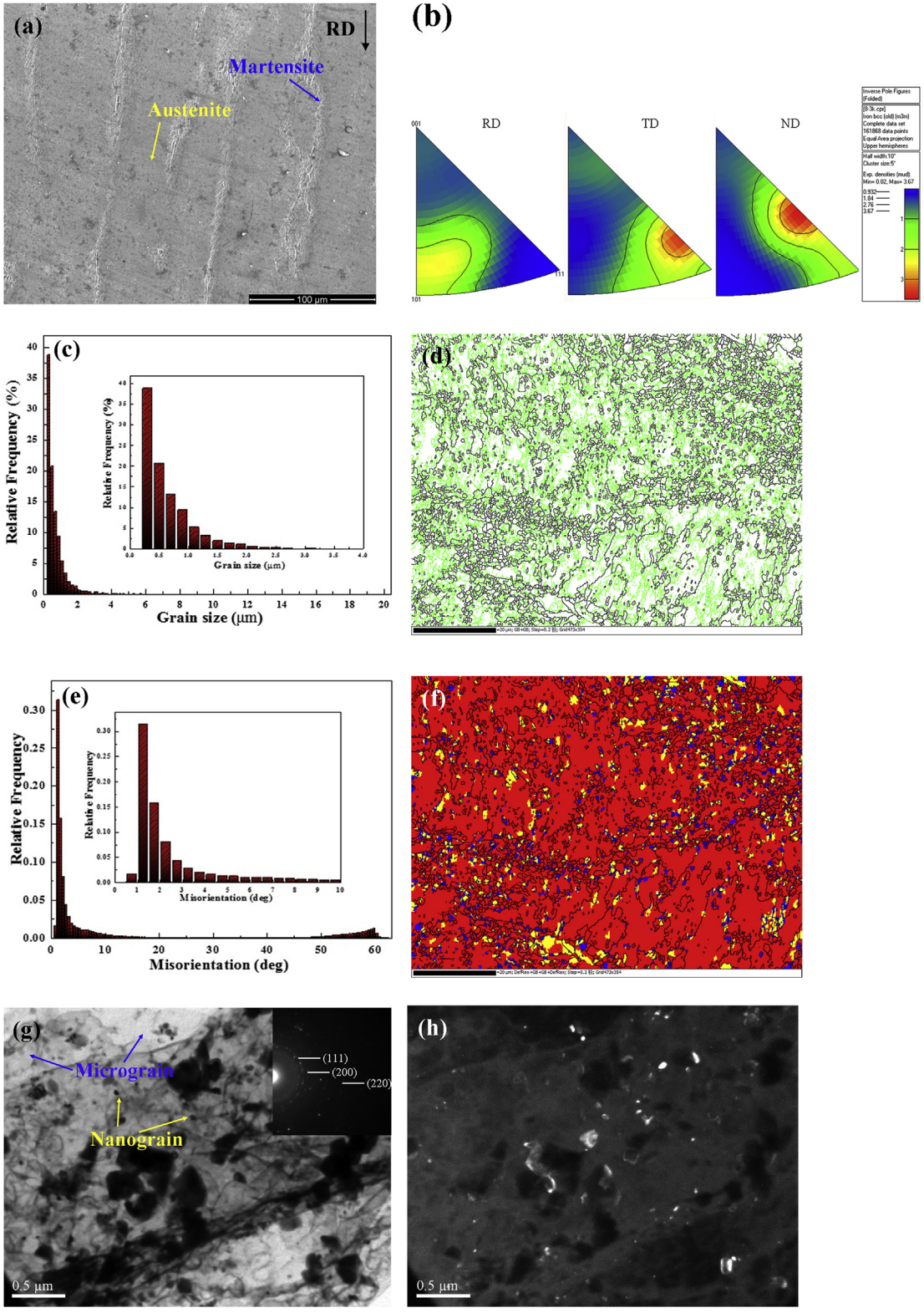

Fig. 5 – Experimental observations of the micro/nano-structured 304 SS (a) SEM image, (b) corresponding inverse pole figure in elliptical area A of Fig. 4(b), (c) grain size distribution of the number of ultrafine grains, (d) EBSD grain boundaries map, green line represented low-angle grain boundaries (2° < misorientation angle ≤15°) and black line represented high-angle grain boundaries (misorientation angle >15°), (e) statistical diagram of grain boundary misorientations, (f) EBSD image for substructures and deformed grain, (g) bright field TEM image (up inset, SAED), (h) dark field TEM image.

nanocrystalline austenite below 100 nm accounted for the majority. There were two sources of these nanocrystalline austenite grains. One was the grain growth of as-cast 304 SS prepared by AR, and the other one was the transformation of martensite into austenite.

3.2. *Unique mechanical responses under uniaxial tension*

Tensile properties of the micro/nano-structured 304 SS at RT and conventional stainless steel were compared, which were illustrated in Fig. 6. Herein, Fig. 6(a) illustrated the uniaxial tensile engineering stress–strain curves of the present work and a reference of the uniform structured conventional 304 SS [27]. Fig. 6(b) showed the corresponding true stress–strain curves. The micro/nano-structured 304 SS showed amazing engineering tensile elongation to fracture (27.3%) even at high yield strength (849 MPa) and ultimate tensile strength (1023 MPa). At the same time, the hardness of specimen was as high as 355 HV (conventional 304 SS only reached 186 HV).

3.3. *Fractography*

By means of SEM observation and analysis for micro fracture morphology, the fracture type was determined, and mechanism of crack formation, propagation and fracture was discussed. Observation of tensile fracture by SEM was shown in Fig. 7. As we could see in Fig. 7(a), martensite region presented predominant cleavage river pattern (yellow rectangle) and the austenite region showed the characteristic of brittle fracture ductile (green rectangle). The content of strain induced martensite were less, the number of tearing cavities between martensite group with smaller diameter and matrix were more, and some large dimples with an average diameter of 7 μm could be observed. Fig. 7(b) was the observation after local magnification of Fig. 7(a). Large number small dimples with an average diameter of only 300 nm could be found around the big dimples. In conclusion, ductile fracture was the main fracture mode as a whole. This indicated that the specimen had good plasticity at RT.

4. Discussion

The microstructure of as cast specimens prepared by AR changed with rolling and annealing. The interaction mechanism in microstructure could overwhelm the reducing mechanical performance. At first, there were high density dislocations entangled with each other in the original structure. When dislocation density was close to saturation, deformation twins would be produced, and content of deformation twins would increase. Finally, deformation induced martensite was produced under the interaction of dislocation and deformation twin. With the progress of rolling deformation, the content of strain induced martensite increased. The driving force of deformation induced martensite was the different of free energy between old and new phases. When the mechanical driving force and chemical driving force were superposed to the critical value of driving force, strain induced martensite would be formed. The diffusion ability of atoms was relatively poor, and the dynamic recovery of deformed metals would be inhibited at RT. Accordingly, high density dislocation, stacking fault and other defects were produced in the rolling process. These defects provided more nucleation sites for martensite nucleation, and strain induced martensite nucleation and growth in high density dislocations and other defects.

The plastic rolling deformation was one method to enhance the microstructure and mechanical characteristics of austenitic stainless steel. The deformation structure of 304 SS slab prepared by AR was mainly composed of strain induced α' martensite and deformed retained austenite. Here, the structure contained high density dislocation, deformation twin, stacking fault and other defects. Due to the existence of martensite and various defects, the stainless steel had high strength and poor plasticity at RT. In order to further improve the mechanical properties, annealing treatment was carried out [28]. Annealing was believed to eliminate the generation of dislocations. Beyond that, the recrystallized ultrafine austenite grains, the restored nanocrystalline austenite transformed from α' to γ, and the residual martensite as well as the composite structure composed of the micro/nano-crystalline austenite contained in as-cast microstructure could be obtained through annealing. This kind of non-uniform composite structure could realize optimal combination of strength and plasticity. The recovery of martensite to austenite and the annihilation of various defects occurred during annealing. In this study, the recovery mechanisms of 304 SS slab were two major types of martensitic shear and diffusion recovery after rolling at RT. The transformation from $\alpha' \rightarrow \gamma$ was mainly realized by the movement of α'/γ interface and the formation of restored austenite [29]. The twin γ was formed through the transformation of $\alpha' \rightarrow \gamma$, and the sub-crystal structure was formed along with the recovery process. In the same way, the specific mechanism of $\alpha' \rightarrow \gamma$ recovery could be studied by thermodynamic calculation method combined with microstructure characteristics. The change of free energy in the process of $\alpha' \rightarrow \gamma$ transformation could be estimated by Eq. (1). The value of $\Delta G_{Fe}^{\alpha' \rightarrow \gamma}$ at the annealing temperature of 973 K could be calculated as −317 J/mol. When the free energy was negative, γ was more stable than α'. Therefore, $\alpha' \rightarrow \gamma$ recovery obviously occurred during annealing. According to the research results of Tomimura [29], diffusion recovery and shear recovery mechanisms existed in the process of martensite recovery during annealing and diffusion recovery mechanism played a leading role. In the shear recovery process, the deformed structure often contained lamellar deformed austenite with high dislocation density, which could be divided into sub crystal and dislocation grain. However, the austenite recovered into the diffusion recovery mechanism was different from that in the equiaxed phase, and grew up with the extension of annealing time, thus consuming the residual martensite. But with prolonging anneal time, these austenite grains would grow into equiaxed grains, and finally form austenite grains with low dislocation density [25,30,31]. In the same way, the nanocrystalline austenite contained in as-cast structure and recovered from martensite after annealing treatment of cold rolling stainless steel had good thermal stability. According to research results of Lu K. [32], this was due to the activation of some

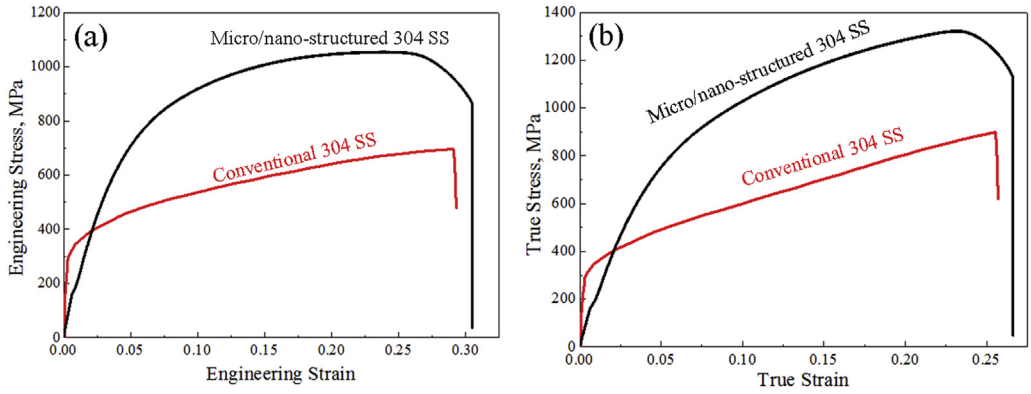

Fig. 6 – Tension curve of the micro/nano-structured 304 SS relation with the uniform structured one (a) engineering stress–strain curves, (b) representative true stress–strain curves.

dislocations by plastic deformation, which resulted in the formation of small angle grain boundaries between nanocrystalline grains. After cold rolling, the small angle grain boundary with austenite grain size less than 15° accounts for 92.4% in the specimen. Thereby, the thermal stability of nanocrystalline boundary was enhanced from high energy state to low energy state. The spontaneous transition from grain boundary to low energy state made the thermal stability of nanocrystalline grains significantly improved. Accordingly, the microstructure of 304 SS in study contained low density dislocations, austenite grains with inhomogeneous distribution of micro/ultrafine/nano grains, and residual α′ martensite [33].

into martensite, and the strengthening effect of martensite was more significant. At this time, the number of ultrafine grains accounted for 67.5%, in which 37% were austenite grains with an average grain size below 300 nm, the average grain size of retained austenite was 1.02 μm, and the small angle grain boundary accounted for 92.4%, among which 51.3% were sub grain boundary below 2°. The hardness and strength of were greatly improved. A large number of defects (dislocation tangle, stacking fault, and twin) were produced in the rolling process, which leaded to the improvement hardening ability. In addition, dynamic recovery and recrystallization were severely inhibited by rolling at RT, which leaded to the maintenance of high dislocation density. These high

$$\Delta G^{\alpha'\to\gamma}(J/mol) = 10^{-2}\Delta G_{Fe^{\alpha'\to\gamma}}(100 - Cr - Ni) - 97.5Cr + 2.02Cr^2 - 108.8Ni + 0.52Ni^2 - 0.05CrNi + 10^{-3}T(73.3Cr - 0.67Cr^2 + 50.2Ni - 0.84Ni^2 - 1.51CrNi) \quad (1)$$

After cold rolling, yield strength and tensile strength were greatly improved, more austenite structure was transformed

strengthening defects could promote nucleation of a part martensitic transformation. With the progress of rolling

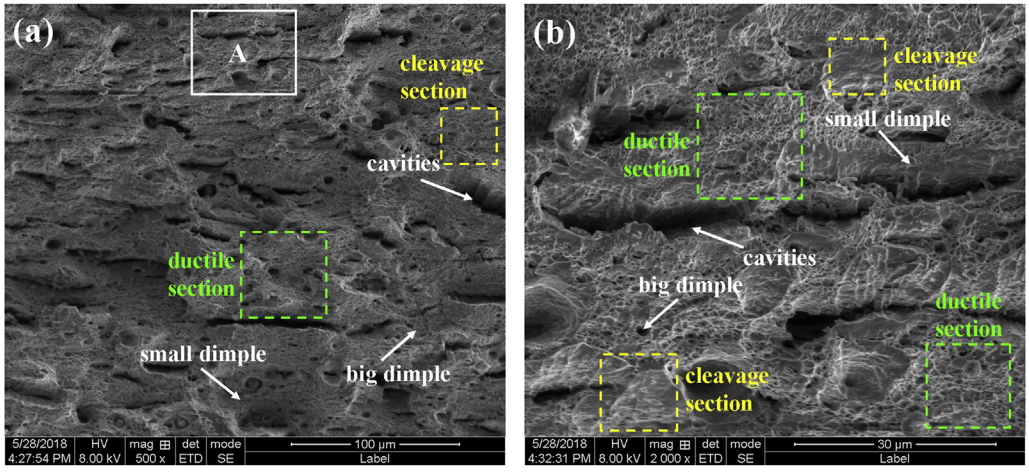

Fig. 7 – Fracture surface morphology of the micro/nano-structured 304 SS (a) SEM images, (b) the area of white rectangle A in (a).

deformation, the accumulated dislocation density reached saturation, and dislocation interaction increased obviously, which resulted in the formation of a large number of deformation twins in austenite matrix. Interaction of these deformation twins provided more nucleation sites for strain induced martensite. With the progress of rolling deformation, the microstructure of martensite became smaller, and some of them were broken.

After annealing for 1 h, the recrystallization of deformed austenite and the recovery of strain induced martensite occurred. The average grain size of ultrafine austenite was 713.8 nm, the volume fraction of ultrafine grains was 82.5%, and the number of grains below 300 nm accounted for 38.8%. The content of nanocrystalline austenite increased due to the recovery of α' strain induced martensite. TEM images indicated that average grain size of the nanocrystalline austenite was about 86 nm, accounting for 21% of its volume fraction. The composite structure of microcrystalline grains/ultra-fine grains/nanocrystalline grains, which was formed with nanocrystalline austenite grains and retained austenite grains. Depending on this, the optimized combination of ultra-high strength and excellent plasticity of 304 SS was realized.

5. Conclusions

Hierarchical structured 304 SS with heterogeneous grains from nanoscale to microscale was prepared via AR. The main conclusions are listed as follows:

(1) With the progress of rolling deformation for 50% at RT, austenite grain size decreased, the content of strain induced martensite and dislocation density increased obviously. Here, heterogeneous composite structure were obtained, which composed of high density dislocation, deformation twin, strain induced martensite and microcrystalline grains/ultra-fine grains/nanocrystalline grains.
(2) After annealing treatment, deformed austenite was recrystallized, defects such as dislocations and twins in deformed austenite were eliminated gradually, content of nanocrystalline austenite was increased, and grain size growth of recrystallized ultrafine and nanocrystalline austenite was not obvious owing to low annealing temperatures.
(3) The excellent combination of strength and plasticity for micro/nano-structured 304 SS was attributed to the obstruction of dislocation by nanocrystalline austenite and residual martensite, as well as high work hardening ability of micro/nano-structured heterogeneous composite structure.

Declaration of Competing Interest

We declared that we have no conflicts of interest to this work. We declare that we do not have any commercial or associative interest that represents a conflict of interest in connection with the manuscript entitled, "Micro/nano-structure leads to super strength and excellent plasticity in nanostructured 304 stainless steel".

Acknowledgments

This work is supported by the National Natural Science Foundation of China (51911530119), Department of Education of Gansu Province Innovation Fund (2021A-023), Open Project Fund of Gansu Key Laboratory of Solar Power System Engineering Project (2021SPEK01) and Scientific Research and Development Guidance Fund of Lanzhou Univerisity of Technology (19062034).

REFERENCES

[1] Duarte MJ, Klemm J, Klemm SO, Mayrhofer KJJ, Stratmann M, Borodin S, et al. Element-resolved corrosion analysis of stainless-type glass-forming steels. Science 2013;341:372–6.
[2] Lo KH, Shek CH, Lai JKL. Recent developments in stainless steels. Math Sci Eng R 2009;65:39–104.
[3] Dywel P, Szczesny R, Domanowski P, Skowronski L. Skoworonski, Stuctural and micromechanical properties of Nd: YAG laser marking stainless steel (AISI 304 and AISI 316). Materials 2020;13:2168.
[4] Fan JT, Zhu LL, Lu J, Fu T, Chen AY. Theory of designing the gradient microstructured metals for overcoming strength-ductility trade-off. Scripta Mater 2020;184:41–5.
[5] Wang SG, Sun M, Liu SY, Liu X, Xu YH, Gong CB, et al. Synchronous optimization of strengths, ductility and corrosion resistances of bulk nanocrystalline 304 stainless steel. J Mater Sci Technol 2020;37:161–72.
[6] Sheng J, Li JC, La PQ, Wei FA, Song Y, Wang KL. Investigating the tensile properties of micro-nanostructured 304 stainless steel with SEM and in-situ tension. Sci Adv Mater 2017;9:1020–7.
[7] Mallick P, Tewary NK, Ghosh SK, Chattopadhyay PP. Microstructure-tensile property correlation in 304 stainless steel after cold deformation and austenite reversion. Mater Sci Eng, A 2017;707:488–500.
[8] Koyama M, Zhang Z, Wang MM, Ponge D, Raabe D, Tsuzaki K, et al. Bone-like crack resistance in hierarchical metastable nanolaminate steels. Science 2017;355:1055–7.
[9] Wang HD, La PQ, Shi T, Wei YP, Lu XF. Research status and development trend of bulk nano/micro-crystalline composite metallic materials. J Mater Eng 2013;41:92–6.
[10] Jiang P, Lu J, Wu XL. Microstructure evolution and tensile properties of 304L stainless steel subjected to surface mechanical attrition treatment. Mater Sci Forum 2010;667–669:175–9.
[11] Liu G, Lu J, Lu K. Surface nanocrystallization of 316L stainless steel induced by ultrasonic shot peening. Mater Sci Eng, A 2000;286:91–5.
[12] Wu XL, Jiang P, Chen L, Zhang JF, Yuan FP, Zhu YT. Synergetic strengthening by gradient structure. Mater Res Lett 2014;2:185–91.
[13] Wu G, Liu C, Sun LG, Wang Q, Sun BA, Han B, et al. Hierarchical nanostructured aluminum alloy with ultrahigh strength and large plasticity. Nat Commun 2019;10:1–8.
[14] Wu XL, Yang MX, Yuan FP, Wu GL. Heterogeneous lamella structure unites ultrafine-grain strength with coarse-grain ductility. P Natl Acad Sci USA 2015;112:14501–5.

[15] Ovid'ko IA, Valiev RZ, Zhu YT. Review on superior strength and enhanced ductility of metallic nanomaterials. Prog Mater Sci 2018;94:462–540.
[16] Huang CX, Hu WP, Wang QY, Wang C, Yang G, Zhu YT. An ideal ultrafine-grained structure for high strength and high ductility. Mater Res Lett 2014;3:88–94.
[17] Valiev RZ, Zhu YT. Recent findings in superior strength and ductility of ultrafine-grained materials. Trans Mat Res Soc Japan 2015;40:309–18.
[18] Wang YM, Chen MW, Zhou FH, Ma E. High tensile ductility in a nanostructured metal. Nature 2002;419:912–5.
[19] Sheng J, Su JQ, La PQ, Ren JQ, Ma JQ, Shi Y, et al. Progess of in-situ study on mechanical properties for micro/nano-structured alloy. J Nanoelectron Optoelectron 2018;13:637–45.
[20] Ma GC, Sheng J, Meng Q, Du MC, La PQ, Zheng YH, et al. Effect of heterogeneous composite structure on the microstructure and properties for nanostructured 2205 duplex stainless steel. Integrated Ferroelectrics Int J 2021;217:190–7.
[21] La PQ, Yang J, Cockayne DJH, Liu WM, Xue QJ, Li YD. Bulk nanocrystalline Fe3Al-based material prepared by aluminothermic reaction. Adv Mater 2006;18:733–7.
[22] La PQ, Wang HD, Yang Y, Bai YP, Wei YP, Lu XF. Effect of annealing on grain size and mechanical properties of bulk nanocrystalline Fe3Al materials with 10% Cr prepared by aluminothermic reaction. Nanotech Precis Eng 2012;10:229–36.
[23] La PQ, Wei YP, Lv RJ, Yang Y. Effect of Mn element on microstructure and mechanical properties of bulk nanocrystalline Fe3Al based materials prepared by aluminothermic reaction. Mater Sci Eng, A 2010;527:2313–9.
[24] Sheng J, La PQ, Su JQ, Ren JQ, Ma JQ, Shi Y, et al. In situ SEM analysis for deformation mechanism of micro/nanostructured 304 stainless steel with high strength and good plasticity. Mod Phys Lett B 2018;32:1850182.
[25] Sheng J, Jing J, Shi Y, Chen WQ, Ma GC, Wei JF, et al. Superior strength and ultrahigh ductility in hierarchical structured 2205 duplex stainless steel from nanoscale to microscale. Mater Trans 2021;62:1604–8.
[26] Wang KL, Song Y, La PQ, Wei FA, Ma FL, Sheng J, et al. Effect if rolling deformation on nanograins and mechanical properties of exceptional nano/microcrystalline 304 stainless steel. Steel Res Int 2018;89:1700490.
[27] Han YJ. The effects and mechanism of rolling and annealing on microstructure and mechanical properties of nanocrystalline/microcrystalline composite 304 austenite stainless steel. Lanzhou Univ Tech; 2017.
[28] Forouzan F, Najafizadeh A, Kermanpur A, Hedayati AH, Surkialiabad R. Production of nano/submicron grained AISI 304L stainless steel through the martensite reversion process. Mater Sci Eng, A 2010;527:7334–9.
[29] Liang GF, Zhu LY, Wang CQ, Nolli P, Wu JC, Yu Y, et al. In-situ observation of $\delta \rightarrow \gamma$ phase transformation of an AISI 304 stainless steel. Acta Metall Sin 2007;43:119–24.
[30] Takaki S. Reversion of deformation induced martensite to austenite and mechanism of ultra grain refining. Tetsu to Hagane 1994;80:529–35.
[31] Somani MC, Juntunen P, Karjalainen LP, Misra RDK, Kyrlinen A. Enhanced mechanical properties through reversion in metastable austenitic stainless steels. Metall Mater Trans A 2009;40:729–44.
[32] Zhou X, Li XY, Lu K. Enhanced thermal stability of nanograined metals below a critical grain size. Science 2018;360:526–30.
[33] Xiong Y, Yue Y, Fan MX, He TT, Fan MX, Ren FZ, et al. Cryorolling impacts on microstructure and mechanical properties of AISI 316 LN austenitic stainless steel. Mater Sci Eng, A 2018;709:270–6.